Available online at www.sciencedirect.com
SCIENCE DIRECT®
Optics Communications 226 (2003) 1–5
OPTICS COMMUNICATIONS
www.elsevier.com/locate/optcom

More on patterns in Mie scattering

M. Xu *, R.R. Alfano

Institute for Ultrafast Spectroscopy and Lasers, New York State Center of Advanced Technology for Ultrafast Photonic Materials and Applications, and Department of Physics, The City College and Graduate Center of City University of New York, New York, NY 10031, USA

Received 21 April 2003; received in revised form 19 August 2003; accepted 21 August 2003

Abstract

The powerlaw patterns in Mie scattering (the normalized light intensity $I(\theta)/I(0)$ vs. the dimensionless qR where $q = 4\pi\lambda^{-1}\sin\frac{\theta}{2}$ is the magnitude of the wave vector transfer at the scattering angle θ for wavelength λ, and R is the radius of the nonabsorbing sphere with a relative refractive index $m > 1$) are analyzed using the geometrical optics approximation for particles of a large size parameter. The $(qR)^{-4}$ powerlaw regime is shown to be present only in Mie scattering of soft particles. The $(qR)^{-2}$ powerlaw regime occurs at the scattering angles of the $p = 1$ geometrical ray (refracted without internal reflections) from the portion of the incident beam with an incidence angle around $\pi/4$ upon the particle. The $(qR)^{-2}$ powerlaw regimes from particles sharing one common relative refractive index but differing in size parameters are collinear. Simple analytical expressions are derived to describe these powerlaw regimes of Mie scattering.

PACS: 3.80.+r; 42.25.Fx; 78.35+c

Keywords: Light scattering; Mie scattering

The study of light scattering by small particles is important in noninvasive characterization of small particles and radiative transfer in turbid media including atmosphere, marine environment and tissues (see, for example, van de Hulst's classic work[1] and the recent review volume edited by Mishchenko, Hovenier and Travis [2]). Light scattering from a sphere of arbitrary size and refractive index (Mie scattering), one of a few exactly solvable cases, was derived in 1908 [3]. This exact solution was given in the form of a slow converging partial-wave series involving complex functions. The physical meaning and interpretation of the Mie scattering was itself of lasting interests [4–7].

Recently, work on powerlaw regimes in Mie scattering was obtained by Sorensen and Fischbach [8] when plotting the normalized light intensity $I(\theta)/I(0)$ versus the dimensionless

* Corresponding author. Tel.: +1-212-650-6865; fax: +1-212-650-5530.
E-mail address: minxu@sci.ccny.cuny.edu (M. Xu).

0030-4018/$ - see front matter
doi:10.1016/j.optcom.2003.08.019

parameter qR, where $q = 4\pi\lambda^{-1}\sin\frac{\theta}{2}$ is the magnitude of the wave vector transfer at the scattering angle θ for wavelength λ after ignoring the interference ripple structure. These patterns were attributed to the structure factor of the illuminated portion of the scattering object. The Fourier transform of the illuminated annular shell for a sphere of radius R was used to explain the emerging $(qR)^0$, $(qR)^{-2}$ and $(qR)^{-4}$ powerlaw regimes. This approach ignores the extra phase shift incurred to the light when it passes through the particle. The implicit assumption made there [8] that the phase shift due to the nonunity refractive index of the particle is negligible is valid for scattering of X-rays [9], but it is inappropriate for optical light scattering from particles with a large phase shift.

In this paper, we analyze patterns in Mie scattering using the geometrical optics approximation (GOA) for particles of a large size parameter and derive simple analytical expressions to describe these powerlaw regimes of Mie scattering.

The increase of the phase shift accompanies with the increase of the size parameter. The GOA becomes a viable one when the size parameter $x = kR \gg 1$ where $k = 2\pi\lambda^{-1}$ is the wave number. The scattering amplitude of light is composed of a diffraction light component and reflected and refracted rays when the contribution from surface waves can be neglected [10,1]. The diffraction peak is highly concentrated around the exact forward direction within angle $\Delta\theta \sim 1/x$. By ignoring the interference ripple structure, the Mie scattering in near forward scattering directions and outside the diffraction peak for soft particles whose refractive index m is close to unity ($|m-1| \ll 1$) and for dense particles ($m \sim 1.5$) in GOA is dominated by the $p = 1$ geometrical ray (refracted without internal reflections) [10–12]. The $(qR)^{-2}$ and $(qR)^{-4}$ powerlaw regimes can be recovered from the asymptotic behavior of the contribution from this $p = 1$ geometrical ray [see Fig. 1].

The magnitude of the scattering amplitude of perpendicular polarization with respect to the scattering plane which was examined in [8] (the parallel polarization case can be analyzed in a

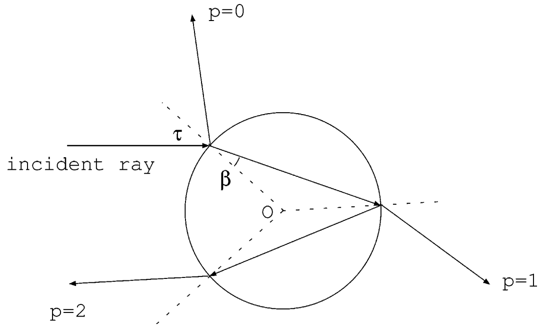

Fig. 1. Geometrical rays scattered by a sphere.

similar fashion) is dominated by the contribution A_{R_1} from the $p = 1$ geometrical ray [10]

$$|S_1(\theta)| \simeq A_{R_1} = \frac{2mx\left(\sqrt{m^2+(m^2-1)t^2}\right)^{3/2}\left(\sqrt{m^2+(m^2-1)t^2}-1\right)}{(m^2-1)^2(1+t^2)^{3/2}\left(\sqrt{m^2+(m^2-1)t^2}+t^2\right)^{1/2}} \tag{1}$$

and the scattering angle θ is expressed as

$$\sin\frac{\theta}{2} = \frac{t\left(\sqrt{m^2+(m^2-1)t^2}-1\right)}{m(1+t^2)} \tag{2}$$

in terms of the incidence angle τ where $t = \tan\tau$.

For soft particles, Eqs. (1) and (2) can be expanded in powers of $\mu \equiv m - 1$

$$A_{R_1} = \frac{x}{2}\left[\frac{1}{1+t^2}\mu^{-1} + 1 + \mathcal{O}(\mu)\right], \tag{3}$$

$$\sin\frac{\theta}{2} = \mu t + \mathcal{O}\left(\mu^2\right), \tag{4}$$

yielding

$$A_{R_1} \simeq \frac{x}{2}\frac{\mu}{\mu^2 + \sin^2\frac{\theta}{2}} \simeq \frac{x}{2}\frac{\mu}{\sin^2\frac{\theta}{2}} \tag{5}$$

under the condition $\mu \ll \sin\frac{\theta}{2} \ll \sqrt{\mu}$. The first approximate form in (5) appeared in the classic book of van de Hulst [1, p. 222].

When $\sin\frac{\theta}{2} \sim \mu$, the incidence angle τ is around $t = \tan\tau = 1$, Eqs. (1) and (2) can also be expanded about this point $t = 1$

$$A_{R_1} = \frac{\sqrt{2}mx}{m^2-1}\left(\frac{\sqrt{2m^2-1}}{\sqrt{2m^2-1}+1}\right)^{3/2} \times \left\{1 - \frac{1}{2}\left[1 + \frac{m^2+1}{\sqrt{2m^2-1}(\sqrt{2m^2-1}+1)} \times \frac{1}{\sqrt{2m^2-1}}\right](t-1)\right\}, \tag{6}$$

$$\sin\frac{\theta}{2} = \frac{\sqrt{2m^2-1}-1}{2m} \times \left\{1 + \frac{1}{2}\left[1 + \frac{1}{\sqrt{2m^2-1}}\right](t-1)\right\}. \tag{7}$$

Since the refractive index $m \sim 1$,

$$\frac{m^2+1}{\sqrt{2m^2-1}(\sqrt{2m^2-1}+1)} \sim 1$$

for soft particles, and the two values inside the brackets of (6) and (7) are close even for dense particles, we find

$$A_{R_1} \simeq \frac{\sqrt{2}x}{\sin\frac{\theta}{2}} \frac{(\sqrt{2m^2-1})^{3/2}}{(\sqrt{2m^2-1}+1)^{5/2}}. \tag{8}$$

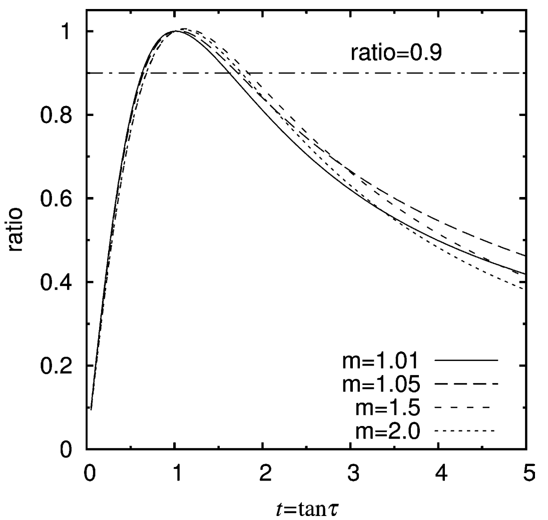

Fig. 2. The ratio $(A_{R_1} \sin\frac{\theta}{2})/(A_{R_1} \sin\frac{\theta}{2})_{t=1}$ versus $t = \tan\tau$. The curves obtained for particles of different refractive indices intersect with the 90% line at $t \simeq 0.7$ and $t \simeq 1.6$ where the value of the incidence angle is $\tau = 0.2\pi$ and $\tau = 0.3\pi$, respectively.

The range of the incidence angle τ over which the above expression (8) is valid can be examined by plotting $(A_{R_1} \sin\frac{\theta}{2})/(A_{R_1} \sin\frac{\theta}{2})_{t=1}$ versus $t = \tan\tau$ [see Fig. 2]. The range of the incidence angle is approximately $0.2\pi < \tau < 0.3\pi$ for soft and dense particles ($1 < m < 2$) when a 10% relative error is allowed. The corresponding scattering angle range is given by

$$\frac{\sqrt{3m^2-1}-\sqrt{2}}{3m} < \sin\frac{\theta}{2} < \frac{\sqrt{35m^2-25}-\sqrt{10}}{7m}. \tag{9}$$

Thus, we can write the normalized scattered light intensity as

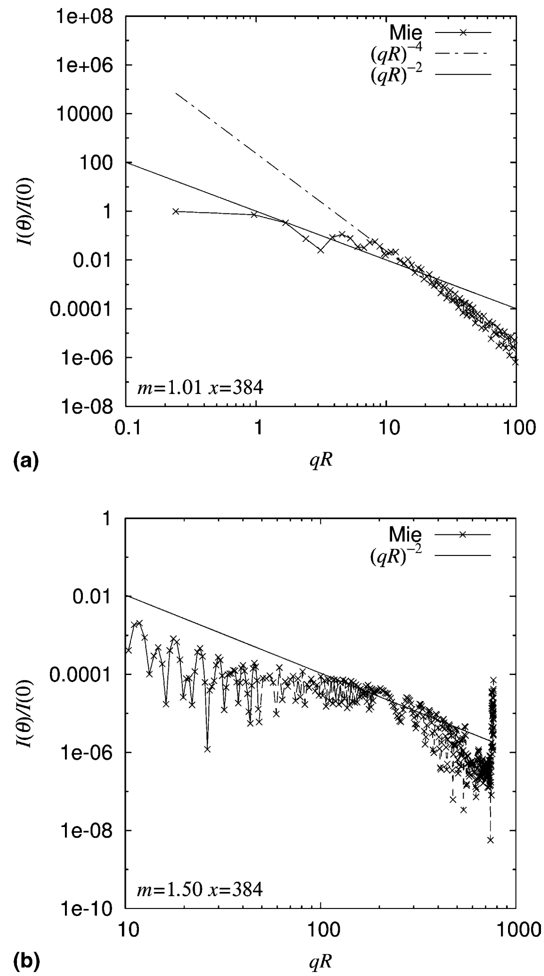

Fig. 3. The powerlaw regimes of a sphere of refractive index: (a) $m = 1.01$; (b) $m = 1.50$. The size parameter is $x = 384$.

$$\frac{I(\theta)}{I(0)}=\frac{|S_1(\theta)|^2}{|S_1(0)|^2} \simeq \begin{cases} \frac{32(\sqrt{2m^2-1})^3}{(\sqrt{2m^2-1}+1)^5}(qR)^{-2} \\ \quad 2k\frac{\sqrt{3m^2-1}-\sqrt{2}}{3m} < q < 2k\frac{\sqrt{35m^2-25}-\sqrt{10}}{7m} \\ 16\mu^2x^2(qR)^{-4} \\ \quad 2k\mu \ll q \ll 2k\sqrt{\mu}, \quad |\mu| \ll 1 \end{cases} \tag{10}$$

from Eqs. (5) and (8) in GOA where we have used the fact $S_1(0)=x^2/2$ and $qR=2x\sin\frac{\theta}{2}$. This shows that the $(qR)^{-2}$ powerlaw regime exists in Mie scattering of both soft and dense particles while the $(qR)^{-4}$ powerlaw regime only appears in soft particles. The $(qR)^{-2}$ powerlaw regimes are collinear while the $(qR)^{-4}$ powerlaw regime are not for particles sharing one common relative refractive index but differing in size parameters. For example, the $(qR)^{-2}$ powerlaw regime is found within $5 < qR < 12$, followed by the $(qR)^{-4}$ powerlaw regime within $8 \ll qR \ll 80$, for a soft sphere of a refractive index $m = 1.01$; only the $(qR)^{-2}$ powerlaw regime is observed within $165 < qR < 300$ for the dense sphere of a refractive index $m = 1.50$ (see Fig. 3). The size parameter of the sphere in both cases is $x = 384$.

Fig. 4 demonstrated the powerlaw regimes for a nonabsorbing sphere with refractive indices

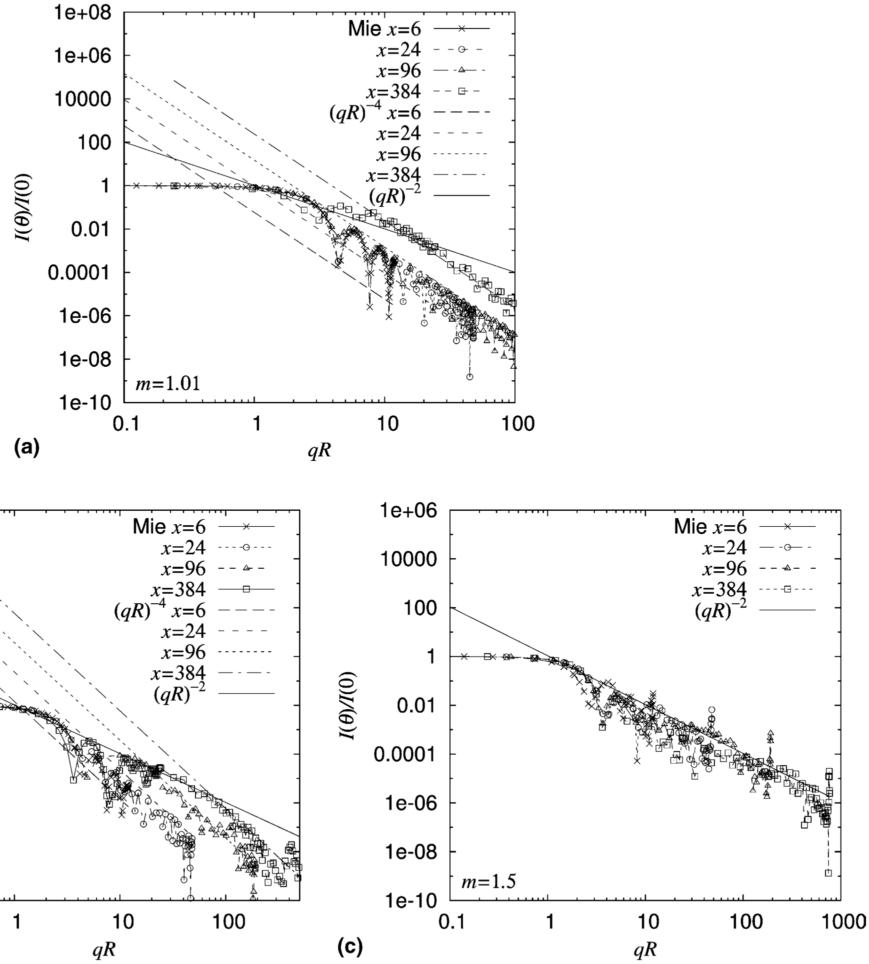

Fig. 4. The normalized Mie scattering curves plotted versus qR for spheres of refractive index: (a) $m = 1.01$; (b) $m = 1.05$; (c) $m = 1.5$. The $(qR)^{-2}$ and $(qR)^{-4}$ powerlaw regimes of Mie scattering given by Eq. (10) are also plotted.

$m = 1.01$, $m = 1.05$ and $m = 1.5$, respectively. The $(qR)^{-4}$ powerlaw regime exists only in soft particles and disappears in dense particles. Its trend agrees well with our simple expression (10) [see the long-dash, dash, dot and dash-dot lines for particles of increasing size parameters in Fig. 4(a) and (b)]. This agreement is better for larger and softer particles. On the other hand, the $(qR)^{-2}$ powerlaw regime exists in both soft and dense particles. This regime occurs at a larger value of qR for particles of a larger size parameter and is broader for denser particles. The $(qR)^{-2}$ powerlaw regimes of particles of a common refractive index but of different size parameters coincide on one straight line (the solid lines in Fig. 4(a)–(c)).

In conclusion, we have analyzed the powerlaw patterns in Mie scattering using the geometrical optics approximation for particles of a large size parameter. The $(qR)^{-4}$ powerlaw regime is shown to be present only in soft particles. The $(qR)^{-2}$ powerlaw regime occurs at the scattering angles of the $p = 1$ geometrical ray (refracted without internal reflections) from the portion of the incident beam with an incidence angle around $\pi/4$ (from 0.2π to 0.3π within a 10% relative error of the scattering amplitude) upon the particle. The $(qR)^{-2}$ powerlaw regimes from particles sharing one common relative refractive index but differing in size parameters are collinear. The $(qR)^{-2}$ and $(qR)^{-4}$ powerlaw regimes of Mie scattering are well captured by the simple analytical expressions given in Eq. (10).

Acknowledgements

This work is supported by NASA and ARMY Medical Commands. One of the authors (M. Xu) thanks the support of the Department of Army (Grant # DAMD17-02-1-0516). The US Army Medical Research Acquisition Activity, 820 Chandler Street, Fort Detrick MD 21702-5014 is the awarding and administering acquisition office.

References

[1] H.C. van de Hulst, Light Scattering by Small Particles, Dover, New York, 1981.

[2] M.I. Mishchenko, J.W. Hovenier, L.D. Travis (Eds.), Light Scattering by Nonspherical Particles: Theory, Measurements, and Applications, Academia Press, San Diego, 1999.

[3] G. Mie, Beitrage zur optik trüber medien speziell kolloidaler metallösungen, Ann. Phys. (1908) 377–445.

[4] H.M. Nussenzveig, W.J. Wiscombe, Efficiency factors in Mie scattering, Phys. Rev. Lett. 45 (1980) 1490–1494.

[5] H. Nussenzveig, Diffraction Effects in Semiclassical Scattering, Cambridge University Press, Cambridge, 1992.

[6] L. Guimaraes, H. Nussenzveig, Theory of mie resonances and ripple fluctuations, Opt. Commun. 89 (1992) 363–369.

[7] A.J. Baran, J.S. Foot, D.L. Mitchell, Ice-crystal absorption: a comparison between theory and implications for remote sensing, Appl. Opt. 37 (12) (1998) 2207–2215.

[8] C.M. Sorensen, D.J. Fischbach, Patterns in Mie scattering, Opt. Commun. 173 (2000) 145–153.

[9] A. Guinier, G. Fournet, C.B. Walker, K.L. Yudowitch, Small-angle scattering of X-rays, John Wiley & Sons, New York, 1955.

[10] A. Ungut, G. han, G. Gouesbet, Comparisons between geometrical optics and Lorenz–Mie theory, Appl. Opt. 20 (17) (1981) 2911–2918.

[11] E.A. Hovenac, Calculation of far-field scattering from nonspherical particles using a geometrical optics approach, Appl. Opt. 30 (33) (1991) 4739–4746.

[12] A. Macke, M.I. Mishchenko, K. Muinonen, B.E. Carlson, Scattering of light by large nonspherical particles: ray-tracing approximation versus *t*-matrix method, Opt. Lett. 20 (19) (1995) 19341936.